Transformation of hematite in diasporic bauxite during reductive Bayer digestion and recovery of iron

Xiao-bin LI, Yi-lin WANG, Qiu-sheng ZHOU, Tian-gui QI, Gui-hua LIU, Zhi-hong PENG, Hong-yang WANG

School of Metallurgy and Environment, Central South University, Changsha 410083, China

Abstract: The reductive Bayer digestion by using iron powder as reductant is proposed to convert hematite to magnetite and further to dissociate iron minerals from sodium aluminosilicate hydrate (desilication product, DSP) based on the differences of their surface properties. The results show that the differences of surface properties between magnetite and DSP in zeta potential, wettability and solvation trend facilitate magnetite to agglomerate, grow up and thus to dissociate from DSP. The increments of reductant amount and alkali concentration favor the transformation of hematite in digestion with the relative alumina recovery of 98.91%. Processing the resultant red mud can obtain qualified iron concentrate with iron grade of approximate 60% and recovery of about 86% through magnetic separation, resulting in reduction of red mud emission higher than 70%. The results are potential to develop a novel technology for processing high iron diasporic bauxite efficiently and provide references for comprehensive utilization of high iron red mud.
Key words: Bayer digestion; reduction; hematite; magnetite; red mud

1 Introduction

The annual output of alumina is estimated to be over 6×10^7 t nowadays in China, resulting in rapid depletion in high A/S (mass ratio of alumina to silica) bauxite. Development and utilization of low A/S, high iron diasporic bauxite with large reserves is of great significance and imperative. This kind of bauxite resource is mainly distributed in Guangxi, Yunnan and many other regions in China with the major characteristics of low Al_2O_3 content (50%−55%), high SiO_2 (~10%) and Fe_2O_3 (20%−30%) contents. In current Bayer digestion with diasporic bauxite, lime (8%−10% mass of ore) needs to be added to accelerate the dissolution of diaspore, and inevitably reacts with the impurity minerals such as hematite, silicate and anatase simultaneously to form insoluble products entering red mud through a series of complex reactions [1]. Correspondingly, the mass fractions of Al_2O_3, SiO_2, Fe_2O_3 and CaO in red mud are 15%−20%, 12%−18%, 30%−50%, 16%−20%, respectively. This denotes that iron and calcium minerals contribute above half of the total mass of red mud, leading to an inevitable large waste emission and the increase of soil salinization and water pollution risk to environment [2,3]. According to the existing technologies, this kind of bauxite cannot be economically processed neither as aluminum resource nor iron resource only. Therefore, it is necessary to recover aluminum and iron comprehensively in treating high iron bauxite. Actually, the economic separation and utilization of iron minerals from bauxite or red mud is a long-term research hotspot, which attracts much attention in the field of alumina production.

There are many methods proposed for separating iron minerals from bauxite or red mud, which can be mainly divided into the following two categories.

1) Direct beneficiation

Methods for recovery of iron minerals by direct ore dressing involve gravity concentration [4], high gradient magnetic separation [5−7], surface magnetization-magnetic separation [8], flotation [9], etc. The effective dissociation and appropriate particle size of iron minerals are required to guarantee the beneficiation effects although these methods are simple. Unfortunately, the iron minerals in bauxite and red mud are always fine-

grained disseminated, leading to either low iron concentrate grade or low iron recovery. For example, industrial practice in Guangxi Branch of CHALCO shows that only 20%−30% iron recovery with concentrate grade of 56% can be obtained by high gradient magnetic separation [10]. This means that it is difficult to reduce the emission of red mud from current Bayer digestion (RM-C) significantly by direct beneficiation.

2) Physical−chemical separation

Bauxite or red mud is heat treated firstly to implement iron minerals conversion and enrichment followed by beneficiation, such as magnetic roasting-separation [11,12] and deep reduction sintering-magnetic separation [13−16]. These methods have favorable separation effects but also have some drawbacks hindering their industrial application such as high energy consumption and relatively complex process.

In short, there exists either low beneficiation effect or high energy consumption in these two kinds of methods. Hence, further study is necessary to develop novel techniques.

Generally, lime is required to eliminate the retardation of anatase on the diaspore digestion and reduce consumption of alkali to a certain degree, but it also brings many adverse effects: 1) causing about 5% alumina loss; 2) increasing 200−300 kg red mud emission per ton of alumina; 3) transforming sodium hydroxide to sodium carbonate by the impurities like $CaCO_3$ in lime; 4) leading to complexity of phase composition and fine-grained dissemination of minerals in red mud, which enhances the difficulty of iron minerals separation.

Our recent studies have shown that, in high pressure Bayer digestion, adding reductant instead of lime can not only ensure alumina recovery [17] but also convert Fe_2O_3 to Fe_3O_4 [18]. These findings may resolve the problems caused by adding lime and benefit iron recovery from red mud. In addition, it is proposed that the formation of Fe_3O_4 is mainly attributed to the reactions in alkaline solution according to formulae (1) and (2).

$$Fe_2O_3 + 2OH^- + 3H_2O = 2Fe(OH)_4^- \tag{1}$$

$$2Fe(OH)_4^- + Fe(OH)_3^- = Fe_3O_4 + 3OH^- + 4H_2O \tag{2}$$

The above studies were conducted in a simple digestion system simulated by using chemicals, and only concerned either substitution of lime or conversion of iron minerals. Specifically, the dissociation and separation of minerals in red mud were not taken into considerations.

Thus, this work focuses on adjusting transformations of minerals in bauxite and mineralogical reconstruction of red mud directionally and synchronously during reductive Bayer digestion process with adding iron powder instead of lime, aiming to accomplish the efficient digestion of diaspore, conversion of hematite to magnetite, and dissociation of iron and silicate minerals in red mud.

2 Experimental

2.1 Materials

Hematite (Sinopharm Chemical Reagent Co., Ltd., China) and iron powder (Tianjin Kemiou Chemical Reagent Co., Ltd., China) were analytical pure, while magnetite was hydrothermally synthesized with hematite (5 g) and iron powder (1 g) under Bayer digestion process conditions (265 °C, 60 min, $\rho(Na_2O_k)$=230 g/L, α_k=3), where Na_2O_k denotes caustic alkali in Na_2O, and α_k is the molar ratio of Na_2O_k to Al_2O_3 in the solution. The kaolin (Hebei Yanxi Minerals Co., Ltd., China) contained 35% Al_2O_3 and 46% SiO_2 according to the chemical components analyses, and mainly consisted of kaolinite and quartz as shown in Fig. 1. Sodium aluminosilicate hydrate (desilication product, DSP) was obtained by kaolin reacting with sodium aluminate solutions ($\rho(Na_2O_k)$=230 g/L, α_k=3, liquid−solid ratio L/S=4) at 265 °C for 90 min. Sodium aluminate solutions were prepared by dissolving aluminum hydroxide (CHALCO, technical grade) and sodium hydroxide (Xinjiang Tianye Group Co., Ltd., China, technical grade) in boiling water.
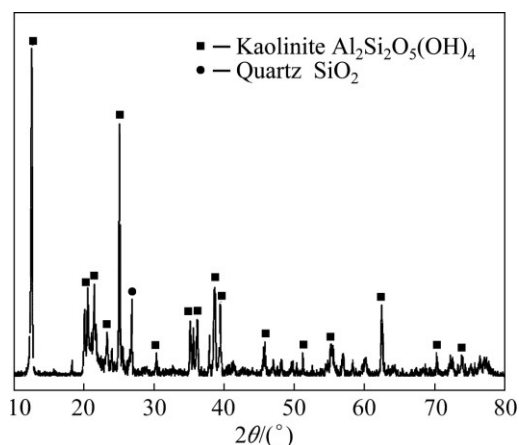
Fig. 1 XRD pattern of kaolin

High iron diasporic bauxite was provided by Guangxi Branch of CHALCO, with the chemical compositions of 51.46% Al_2O_3, 23.93% Fe_2O_3, 6.77% SiO_2 and 3.92% TiO_2 (mass fraction). The mineralogical analysis (Fig. 2) indicates that the main minerals in the bauxite are diaspore, hematite, kaolinite, halloysite, quartz and anatase. The average particle size (d_{50}) of the bauxite is 30.38 μm.

2.2 Charaterization of samples

The zeta potential, magnetic hysteresis loop and contract angle of hematite, magnetite and DSP were determined using potentiometric analyzer (MPT−2, Malvern Instruments, UK), vibrating sample magneto-meter (VSM, HH−15, Nanjing NanDa Instrument Plant, China) and contact angle measurement instrument (CL200B, Shanghai Suolun Instruments, China), respectively. Surface microscopic morphology and micro area composition analyses were conducted by SEM (JSM−6360LV, JEOL, Japan) and EDX (GENSIS60S, EDAX, USA). The mineral phases were identified by XRD (TTR-III, Rigaku Corporation, Japan) using Cu K_α radiation at a scan rate of 10 (°)/min.
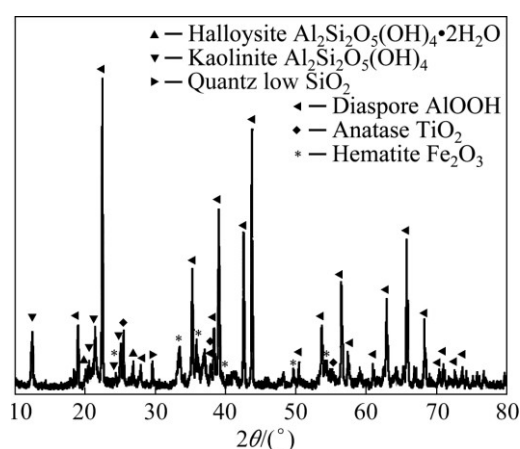
Fig. 2 XRD pattern of high iron diasporic bauxite

2.3 Reductive Bayer digestion

25 g high iron diasporic bauxite, 100 mL sodium aluminate solution and certain mass of iron powder were added into a 150 mL sealed rotating steel bomb immersed in mixed nitrate molten salt cell (XYF−d44×6, Machinery Plant affiliated to Central South University, China) with a preset temperature of 270 °C. The addition amount of iron powder was determined according to the mass ratio of iron powder to bauxite. 2×d15 mm and 4×d5 mm steel balls were put into the bomb in order to strengthen stirring. After 90 min, the bomb was taken out of the molten salt cell and then placed in cold water immediately. The obtained slurry was subsequently filtered and the filter cake was washed with hot water and then dried at 50 °C to obtain the red mud for analyses. The relative alumina recovery was calculated with Eq. (3):

$$\eta_r(Al_2O_3) = \frac{(A/S)_1 - (A/S)_2}{(A/S)_1 - 1} \times 100\% \tag{3}$$

where $\eta_r(Al_2O_3)$ is the relative recovery of alumina, $(A/S)_1$ and $(A/S)_2$ are the mass ratios of alumina to silica in bauxite and red mud, respectively.

2.4 Minerals separation

Magnetic separation was performed on the slurry of red mud at L/S of 15 using a magnetic separator (SSC, Tangshan Hongda Machinery Plant, China) by one roughing operation and one cleaning operation at 0.33 T. The iron concentrate and tailing were filtered and dried for analyses. The iron recovery was calculated based on the iron content and mass of tailing as Eq. (4).

$$\eta(Fe) = \left(1 - \frac{TFe_4 m_4}{TFe_1 m_1 \dfrac{m_3}{m_2}}\right) \times 100\% \tag{4}$$

where $\eta(Fe)$ is the recovery of iron in bauxite, m_1, m_2, m_3, and m_4 represent the masses of bauxite, red mud, separation sample and tailing, respectively. TFe_1 and TFe_4 denote the iron contents in bauxite and tailing, respectively.

The gravity concentration of red mud was preliminarily evaluated. A certain mass of red mud and water were fully mixed in a beaker (L/S=50), then the upper suspension was dumped after apparent stratifying of the slurry, water was added to the underlying slurry to keep the total volume constant and the above operations were repeated 5 times. The underlying slurry and total upper suspensions were filtered and dried separately for analyses, and the iron recovery was also calculated with Eq. (4).

3 Results and discussion

3.1 Surface properties of minerals treated by Bayer digestion process

Iron minerals in current Bayer red mud produced by adding lime exist mainly in the form of fine-grain hematite disseminating with DSP generated by silicate minerals in bauxite reacting with sodium aluminate solutions. However, $Fe(OH)_3^-$ reacts with titanium minerals to form titanium iron compounds when iron powder is added in reductive Bayer digestion, which avoids forming the compact membrane of sodium titanate on diaspore. Therefore, iron powder may replace lime to ensure the digestion effect of diasporic bauxite [17] and simultaneously promote the conversion of hematite in bauxite to magnetite [18]. The growth behaviors of iron minerals and DSP particles are different because of their characteristic surface properties and crystal structures. Amplifying these differences may enhance the dissociation of iron and silicate minerals from one another in digestion, which benefits the effective separation of iron minerals from red mud. Therefore, it is necessary to study the related properties of magnetite, hematite and DSP treated by Bayer digestion process.

The saturation magnetization (*M*) which represents magnetized state of materials in magnetic field is an important characteristic magnet parameter of ferromagnetic substance. The magnetic susceptibilities of magnetite and hematite were measured by VSM and the magnetic hysteresis loops were shown in Fig. 3. The saturation magnetization of hematite treated by Bayer digestion at 265 °C is only 2.37 A·m²/kg, demonstrating that the magnetism of hematite is very weak. While the saturation magnetization of magnetite converted from hematite by adding iron powder is 103.97 A·m²/kg, which shows that magnetite has typical ferrimagnetism. The results suggest that the conversion of hematite to magnetite in digestion can significantly enhance the magnetic property of iron minerals, laying the foundation for the separation of iron minerals in weak magnetic field from the red mud produced by reductive Bayer digestion.
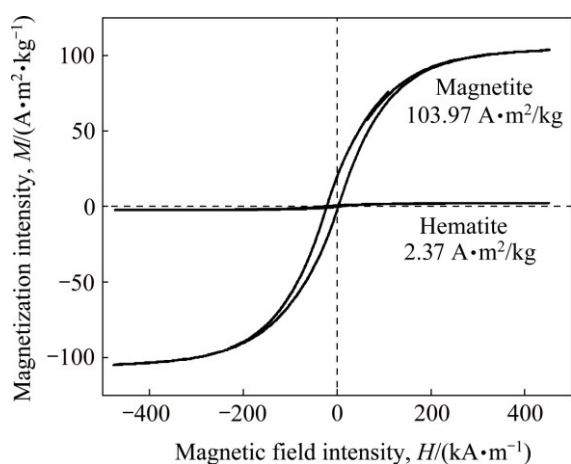
Fig. 3 Magnetic hysteresis loops of hematite and magnetite

The zeta potentials of hematite, magnetite and DSP were further surveyed at different pH to explore their interactions and the results were presented in Fig. 4. All the absolute values of surface potential of hematite, magnetite and DSP increase with the rise of pH. In strong alkaline solution, the zeta potentials of three minerals are all negative and their absolute value order is hematite < magnetite < DSP. Generally, zeta potential represents the electric double layer thickness and charge state (positive or negative) of mineral particle surface. The higher the absolute value of zeta potential is, the thicker the electric double layer is, and the greater the repulsive force among particles with the same charge is. That is, the reunion ability of different mineral particles with the same charge increases with the augment of the zeta potential difference value, and vice versa. Therefore, according to the difference of zeta potential, the repulsive force between DSP and magnetite particles is greater than that of DSP and hematite particles in Bayer digestion process, which favors the growth of mono mineral particles and the increase of mineral

dissociation. Furthermore, it is presumed that the formation of $Fe(OH)_4^-$ by reaction of Fe_2O_3 and OH^- on the hematite particle surface may locally lead to the pH diminution and even to weak acidity, and then the zeta potential may become positive. This means that the hetero-aggregation between positively charged hematite particles and negatively charged DSP particles would take place more readily.
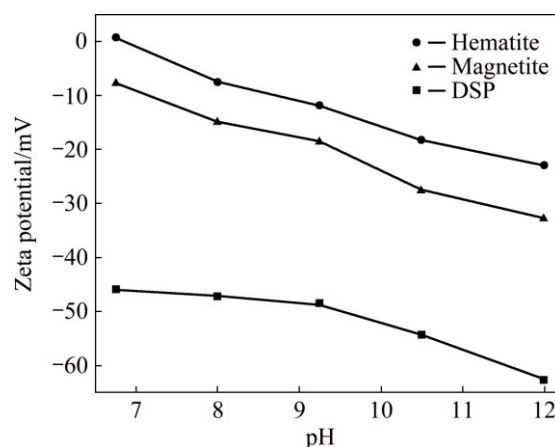
Fig. 4 Zeta potentials of hematite, magnetite and DSP at different pH

The hetero-aggregation and dissemination between DSP and iron minerals particles in digestion are also influenced by the solvation trend and wettability of minerals in solvent. The glycerol (polarity) and diazomethane (nonpolar) were adopted to measure the contact angles of magnetite, hematite and DSP minerals, and the surface free energies were calculated correspondingly by Eqs. (5)−(7). The powder samples were tableted to flakes with a diameter of 1 cm before measurement. Related basic data of glycerol and diazomethane, the contact angles and surface free energies were listed in Tables 1 and 2.

$$\gamma_{L1}(1+\cos\theta_1)=2(\gamma_S^D\gamma_{L1}^D)^{1/2}+2(\gamma_S^P\gamma_{L1}^P)^{1/2} \tag{5}$$

$$\gamma_{L2}(1+\cos\theta_2)=2(\gamma_S^D\gamma_{L2}^D)^{1/2}+2(\gamma_S^P\gamma_{L2}^P)^{1/2} \tag{6}$$

$$\gamma_S=\gamma_S^D+\gamma_S^P \tag{7}$$

where γ_L^D is the liquid dispersion force, γ_L^P is the liquid polarity force, γ_L is the liquid surface free energy, γ_S^D is the solid dispersion force, γ_S^P is the solid polarity force and γ_S is the solid surface free energy.

From Table 2, the contact angles of glycerol on the surface of DSP and hematite are 21.81° and 20.09°, respectively. Their approximate contact angles being less than the contact angle on the surface of magnetite (31.51°) demonstrate that the wettability of magnetite in polar solvent is worse than that of DSP and hematite. LI [19] reported that the solvation trend of mineral augments with the increment of polarity force to dispersion force ratio (γ_S^P/γ_S^D). It can be inferred that the

Table 1 Surface free energies of tested liquids

Tested liquid	γ_L^P /(mN·m^{-1})	γ_L^D /(mN·m^{-1})	γ_L /(mN·m^{-1})	γ_L^P/γ_L^D	Polarity
Glycerol	26.4	37.5	63.9	0.71	Polar
Diazomethane	2.3	48.5	50.8	0.05	Non-polar

Table 2 Average contact angles of test liquids on minerals and surface free energy

Sample	Average contact angle/(°)		γ_S^P /(mN·m^{-1})	γ_S^D /(mN·m^{-1})	γ_S^P/γ_S^D	γ_S/(mN·m^{-1})
	Glycerol	Diazomethane				
DSP	21.81	20.8	21.47	36.58	0.59	58.05
Hematite	20.09	8.36	19.38	39.65	0.49	59.03
Magnetite	31.51	14.01	14.41	40.44	0.36	54.85

solvation trend in polar solvent decreases in the order of DSP, hematite and magnetite, disclosing that magnetite particles are more readily to aggregate and grow up than hematite and DSP particles in Bayer digestion process.

Compared with hematite, the results above show that there are more obvious differences between magnetite and DSP in surface properties such as wettability, surface free energy and solvation trend as well as magnetic properties, but a smaller difference exists in zeta potential. Thus, it can be convinced that the conversion of hematite to magnetite in digestion favors the dissociation of iron and silicate minerals.

3.2 Experimental verification on hetero-aggregation of iron and silicate minerals

The crystallization and dissociation of iron and silicate minerals in digestion process are tightly related to the surface properties of hematite, magnetite and DSP. In order to examine the influence, the hematite, magnetite and DSP samples mentioned in Section 2.1 were identified by X-ray diffraction for minerals composition (Fig. 5) and observed by SEM for microscopic morphology (Fig. 6). The hematite particles (Fig. 6(b)) treated by Bayer digestion are nearly spherical and the particle size obviously becomes finer contrasted with the initial hematite sample (Fig. 6(a)), owing to the dissolution and re-precipitation of hematite in alkali solution [20]. The magnetite particles converted by hematite in reductive Bayer digestion process are octahedral, as shown in Fig. 6(c) and the particles are obviously coarser than that of hematite in granularity (Fig. 6(b)). The magnetite particles have both high crystallinity degree and significant aggregation behavior, caused probably by the high gradient effect between fine magnetite particles [8]. Nevertheless, the DSP particles (Fig. 6(d)) are very fine in granularity and adhesion among particles occurs.

Based on cognizing single mineral reaction behavior above, the disseminating characteristics of iron minerals and DSP were further investigated. The results

show the microscopic morphology and phase composition of products obtained from the mixtures of hematite (10 g) and kaolin (5 g) reacting with 100 mL Bayer solution (ρ(Na$_2$O$_k$)=230 g/L, ρ(Al$_2$O$_3$)=126 g/L) at 260 °C for 90 min in the absence and presence of iron powder (1 g), as demonstrated in Figs. 7 and 8, respectively. The spectral analyses of the micro area on minerals surface are listed in Table 3.
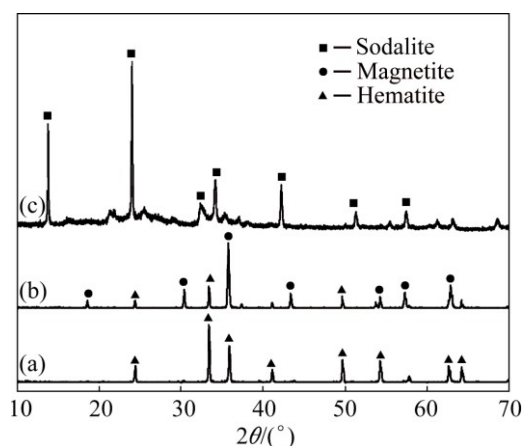
Fig. 5 XRD patterns of hematite (a), magnetite (b) and DSP (c)

In the absence of iron powder (Fig. 7), the product consists of hematite and DSP according to X-ray diffraction pattern. SEM analyses results further reveal that hematite and DSP particles coexist and poorly dissociate, being fine-grain disseminated in product. Moreover, according to EDX results in Table 3, the iron to silicon mass ratios in micro areas *A* and *B* are about 2 and 6, respectively, and initial ratio of original material is 6.08. That is, there exist hetero-aggregations between hematite and DSP particles in Bayer digestion process. Whereas, in the presence of iron powder (Fig. 8), the predominant iron mineral in product is octahedral magnetite converted from hematite and silicate mineral also exists in the form of sodium aluminosilicate hydrate. Being different significantly from Fig. 7, Fig. 8 shows the obvious interfaces among particles after reductive
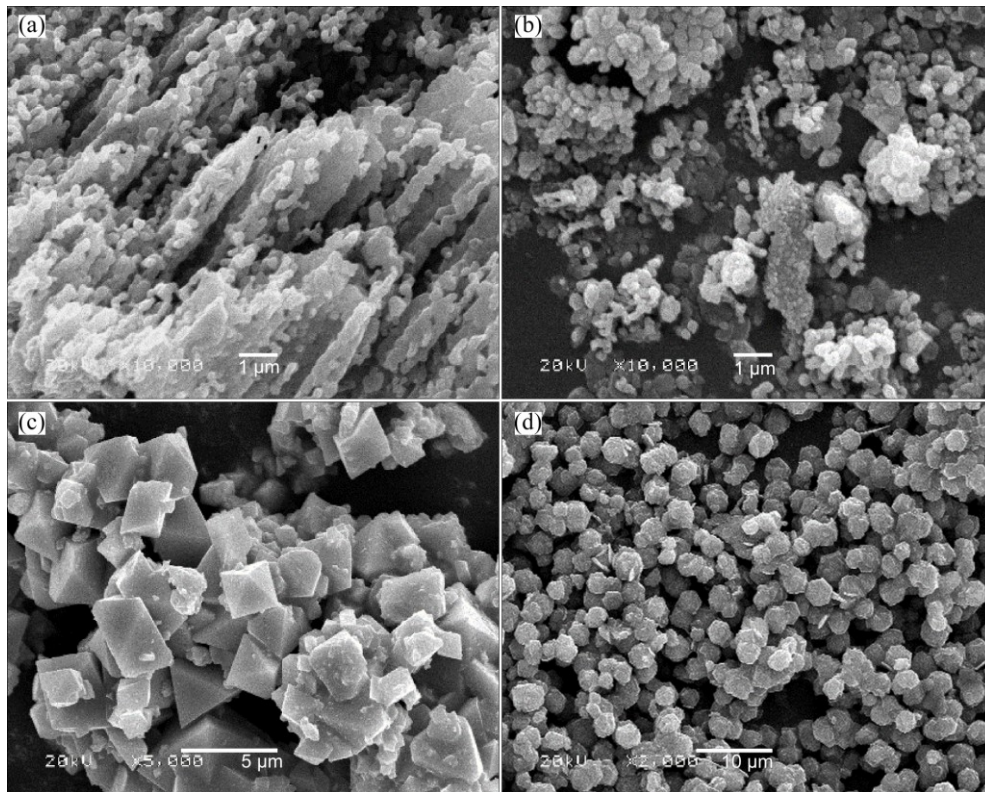
Fig. 6 SEM images of hematite (a (initial), b), magnetite (c) and DSP (d)
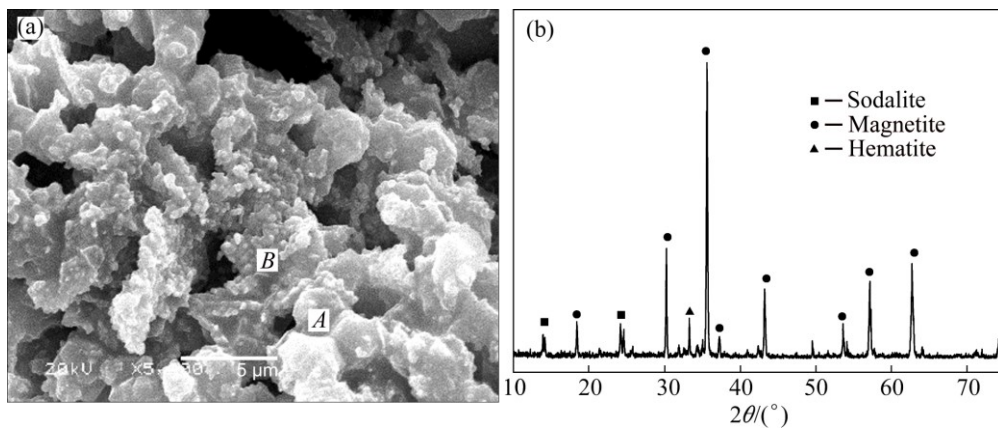
Fig. 7 SEM image (a) and XRD pattern (b) of products obtained from mixtures of hematite (10 g) and kaolin (5 g)
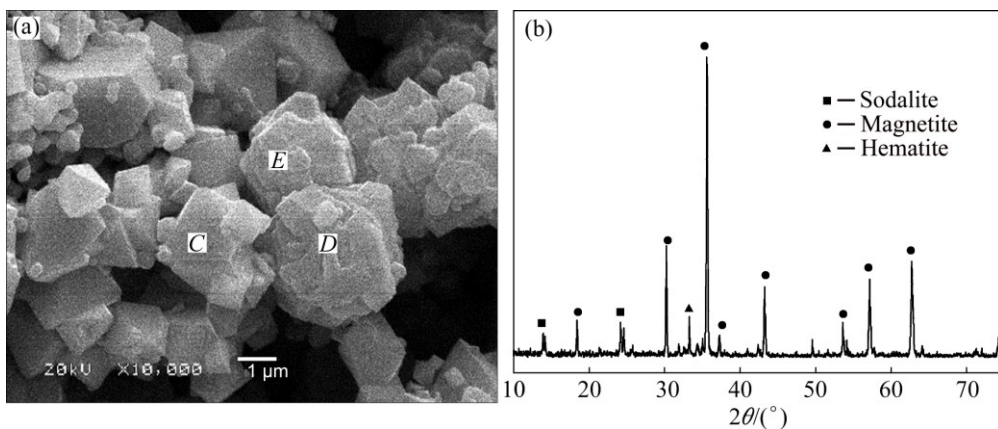
Fig. 8 SEM image (a) and XRD pattern (b) of products obtained from mixtures of hematite (10 g), iron powder (1 g) and kaolin (5 g)

Bayer digestion, implying a possible high dissociation degree. Based on the EDX results in Table 3, it can be further illustrated that the iron to silicon mass ratio in micro area C (~33) is much larger than those in micro areas D and E (~1), all of them are quite different with the initial ratio of 7. Hence, it is regarded as separate existence of magnetite and DSP due to their weak interactions.

Table 3 Micro area composition analyses of mixtures of iron minerals and DSP

Area	Mass fraction/%				
	O	Na	Al	Si	Fe
Fig. 7-*A*	15.93	15.01	19.47	16.37	33.22
Fig. 7-*B*	10.81	9.54	11.18	9.78	58.69
Fig. 8-*C*	4.29	2.25	4.04	2.58	86.84
Fig. 8-*D*	12.54	18.02	23.58	20.91	24.95
Fig. 8-*E*	13.44	18.10	24.46	21.82	22.18

Overall, it can be assumed that the DSP particles stick to hematite particles more readily than to magnetite particles. The dissociation behaviors of iron and silicate minerals are bound up with different surface properties of hematite, magnetite and DSP, which agrees with the discussion in Section 3.1. Therefore, the conversion of hematite to magnetite in reductive Bayer digestion can significantly reduce the fine-grain disseminated degree between iron and silicate minerals and favors the separation of iron minerals from red mud.

3.3 Conversion of iron minerals in reductive Bayer digestion of diasporic bauxite

Recent research on the reaction of hematite in alkaline solution has shown that the increase of temperature, digestion duration and alkali concentration can promote the conversion of hematite to magnetite [18]. In current industrial practice, the Bayer digestion of diasporic bauxite is usually operated at 250−270 °C for 60−90 min, i.e., the adjustment ranges are restricted.

Consequently, the alteration of alkali concentration and the addition amount of iron powder are particularly important to the iron mineral transformation. Figure 9 shows the XRD patterns for red mud from reductive Bayer digestion (RM-R) of diasporic bauxite at 270 °C for 90 min with 230 g/L alkali concentration solution (α_k=3.0) in the presence of 2%−10% iron powder, while Fig. 10 represents the XRD patterns for red mud obtained with 230−250 g/L alkali concentration solution (α_k=3.0) in the presence of 6% iron powder. The solutions consist of sodium carbonite of 17.1 g/L and sodium sulfate of 11.5 g/L.

From Fig. 9, the characteristic peaks of diaspore cannot be observed in the XRD patterns of RM-R, which indicates that diaspore in bauxite is digested completely.

DSP in red mud exists in the form of cancrinite due to the existence of sodium carbonate. In addition, with the increase of iron powder amount, the relative content of magnetite rises and that of hematite correspondingly declines, meaning that the reductant amount has a great effect on the transformation of iron minerals.
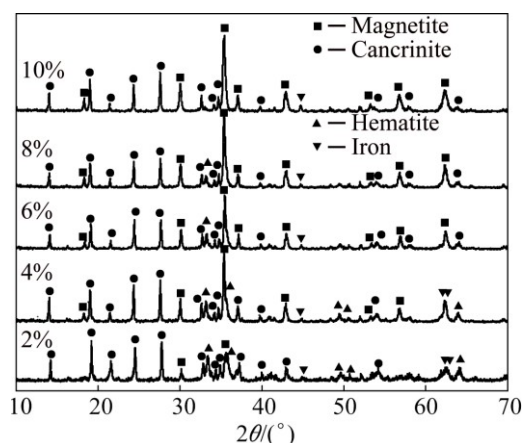
Fig. 9 XRD patterns showing influence of iron powder amount on phase transition of iron minerals ($\rho(Na_2O_k)$=230 g/L)

The iron content in bauxite is about 16.74% and mainly exists as hematite. Only addition amount of iron powder of 2.1% is needed theoretically for the complete conversion of hematite to magnetite, which was verified in preliminary research using pure minerals [18]. However, the diffraction peaks of hematite appeared in the XRD pattern of red mud with iron powder up to 8% and disappeared with iron powder of 10% at $\rho(Na_2O_k)$ of 230 g/L. On the one hand, a part of $Fe(OH)_3^-$ reacts with titanium mineral, forming titanium iron compounds to eliminate the retardation of sodium titanate. On the other hand, the impurity minerals in bauxite, such as silicate minerals, may have an adverse effect on the conversion of hematite, which should be investigated in the future. Furthermore, with the increase of alkali
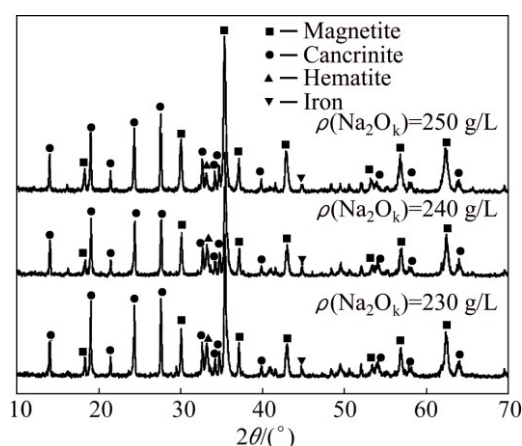
Fig. 10 XRD patterns showing influence of alkali concentration on phase transition of iron minerals (6% iron powder)

concentration, the intensities of diffraction peaks of hematite decline in Fig. 10, suggesting that alkali concentration also affects the conversion of hematite to magnetite. The reason may be that, the equilibrium concentration of both $Fe(OH)_3^-$ and $Fe(OH)_4^-$ is improved with the rise of alkali concentration, promoting the transformation of hematite [21,22]. However, the diffraction peaks of hematite were observed even at alkali concentration of 250 g/L, which demonstrates that hematite is difficult to transform completely only through the adjustment of alkali concentration.

3.4 Separation of iron minerals in RM-R

There exist hematite, calcite, katoite, sodium hydroxide, cancrinite except the unreacted diaspore in RM-C (Fig. 11(a)) with lime added. In contrast, there are only magnetite and cancrinite detected in the RM-R (Fig. 11(b)) with iron powder added, which means that the phase composition of red mud is simplified. It should be noted that the characteristic diffraction peaks of titanium minerals cannot be discerned, possibly due to their amorphous crystallinities. The VSM analyses (Fig. 12) further illustrate that the saturation magnetization of RM-C is only 0.286 A·m²/kg, whereas RM-R shows a typical ferrimagnetism (M=32.13 A·m²/kg),
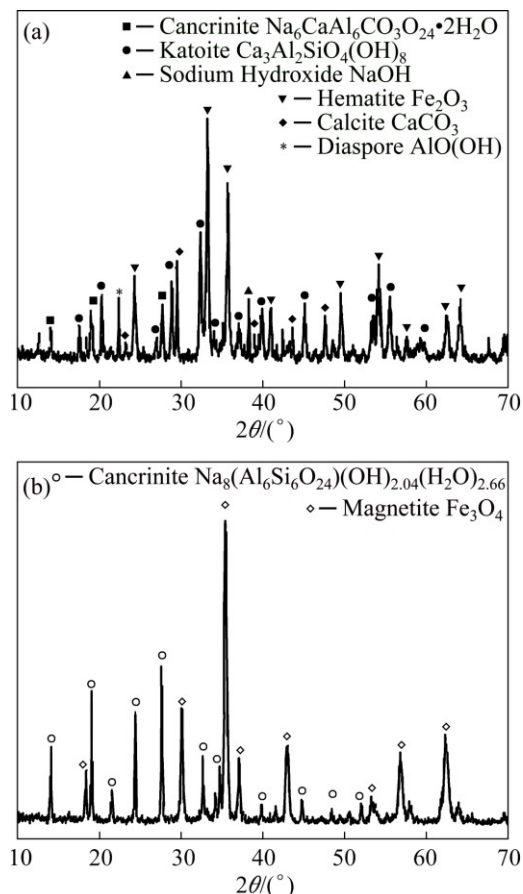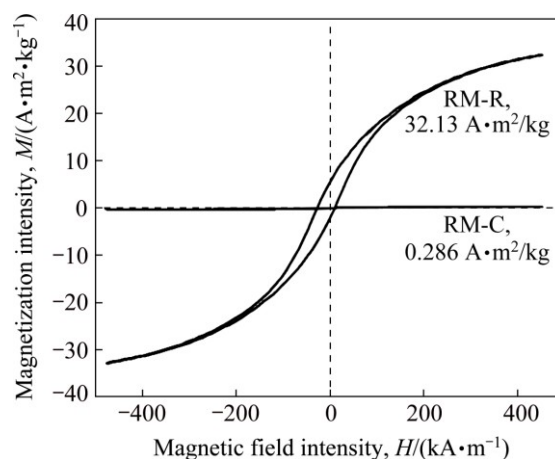
Fig. 12 Magnetic hysteresis loop of RM-C and RM-R

signifying that reductive Bayer digestion benefits the iron recovery from the red mud.

Figures 13 and 14 show the SEM and EDX results of polished samples of RM-C and RM-R, respectively. The dark gray particles in Fig. 13 mainly containing sodium, aluminum, silicon and calcium are composed of minerals such as DSP and katoite; whereas the bright white particles mainly containing iron should be hematite, combined with Fig. 11(a). As shown in different magnification figures, the particles of hematite and other minerals in red mud are mainly wrapped or fine-grain disseminated, and the relatively independent hematite particles cannot be observed. Therefore, satisfactory iron separation results cannot be achieved for treating RM-C through existing beneficiation methods.

In Fig. 14, the off-white particles with main composition of iron and diameter of about 50 μm are magnetite on the basis of result in Fig. 11(b), while the dark gray fine particles are mainly DSP. Compared with RM-C, it's worth noting that the majority of magnetite and DSP particles in RM-R are independent. Consequently, the conversion of hematite to magnetite is conducive to the dissociation of iron minerals and DSP, being accordance with the discussion results for the effects of surface properties on minerals dissociation in Section 3.1. The influence of iron mineral transformation on the iron recovery from red mud was further verified by magnetic separation or gravity concentration experiments.

The results of beneficiation experiments were listed in Table 4. Exp.1 shows that the hematite in RM-C cannot be recovered at low magnetic field strength (0.33 T). However, the magnetite in RM-R with 10% iron powder at $\rho(Na_2O_k)$ of 230 g/L (Exp. 2) can be efficiently recovered under the same conditions, the output rate of concentrate is 70.82% with iron content in concentrate of 60.35% and iron recovery of 86.57%, meanwhile the content of iron in tailing is only 13.66%.

Fig. 11 XRD patterns of RM-C provided by Guangxi Branch of CHALCO (a) and RM-R (b)
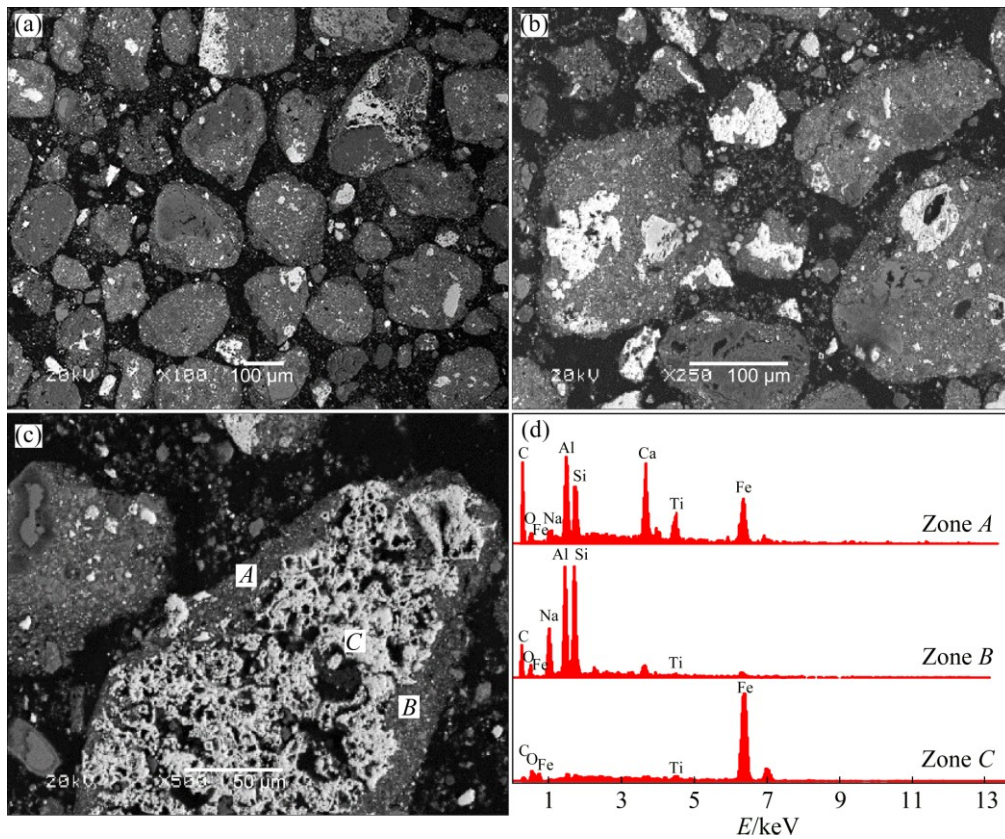
Fig. 13 SEM images (a−c) and EDX spectrum (d) of RM-C provided by Guangxi Branch of CHALCO
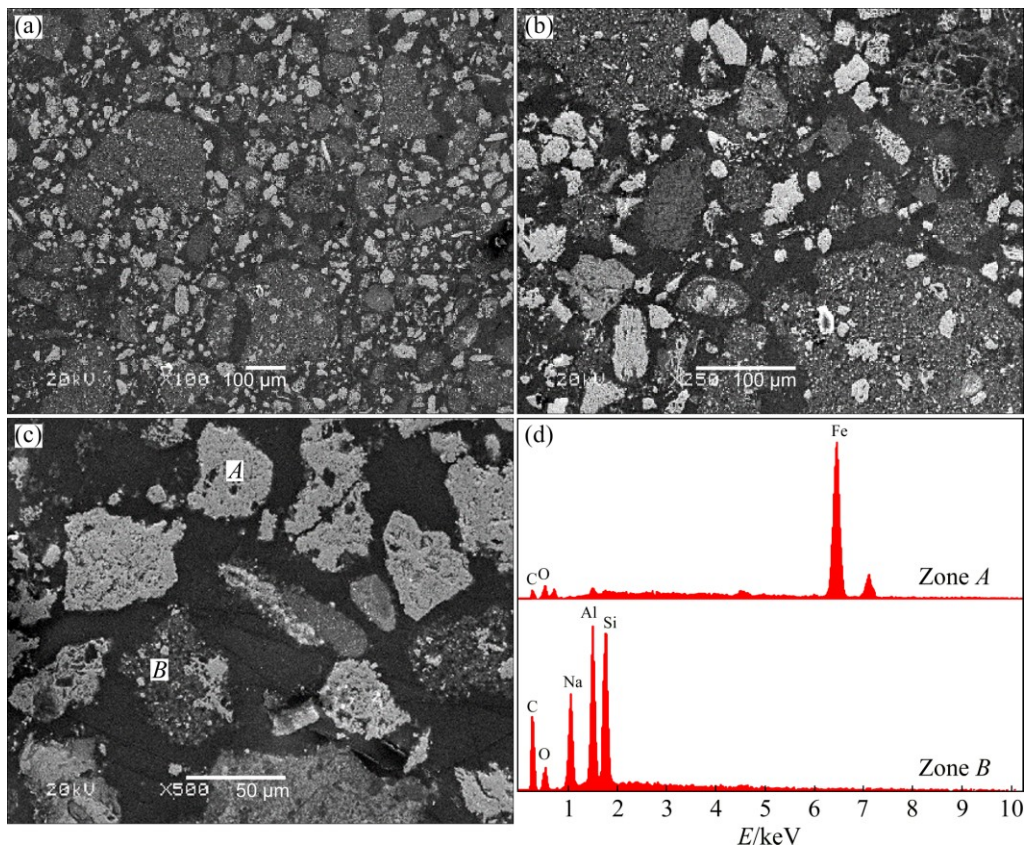
Fig. 14 SEM images (a−c) and EDX spectrum (d) of RM-R (10% iron powder dosage, 270 °C, 90 min, $\rho(Na_2O_k)$=230 g/L, α_k=3.0, 25 g bauxite /100 mL solution)

Table 4 Results of separation of iron minernals from red muds

Exp. No.	Additive	Mass of red mud/g	$w(Al_2O_3)$/%	$w(SiO_2)$/%	$\eta_r(Al_2O_3)$/%	Product	Yield/%	Fe-grade/%	$\eta(Fe)$/%
1	8% CaO	13.76	17.68	11.57	92.00	Concentrate	0	−	0
						Tailing	100	30.3	100
						Sum	100	−	100
2	10% iron powder	14.28	10.76	10.04	98.91	Concentrate	70.82	60.35	86.57
						Tailing	29.18	13.66	13.43
						Sum	100	−	100
3	6% iron powder	12.93	12.45	11.27	98.41	Concentrate	67.10	59.50	86.56
						Tailing	32.90	13.19	13.44
						Sum	100	−	100
4	6% iron powder	12.93	12.45	11.27	98.41	Concentrate	61.10	60.60	78.24
						Tailing	38.90	17.65	21.76
						Sum	100	−	100

Exps. 1−3−Magnetic separation (0.33 T); Exp. 4−Gravity concentration; Digestion conditions: 270 °C, 90 min; 25 g bauxite/100 mL solution; Exps. 1, 2−$\rho(Na_2O_k)$=230 g/L; Exps. 3, 4−$\rho(Na_2O_k)$=250 g/L, α_k=3.0

The similar results can be obtained with $\rho(Na_2O_k)$ increases to 250 g/L while the addition amount of iron powder reduces to 6% (Exp. 3). Exp. 4 in Table 4 is the preliminary evaluation result of gravity concentration of RM-R. The results of gravity concentration are slightly poorer than that of magnetic separation, the iron content in tailings is 17.65% and the iron recovery is 78.24% with iron grade of 60.60% in concentrate. Therefore, intensifying the transformation of hematite to magnetite in reductive Bayer digestion is of significance for the recovery of iron minerals from red mud.

In addition, the chemical compositions of RM-C and RM-R in Table 4 show that the alumina digestion efficiencies are obviously different. When 8% lime, 6% and 10% iron powder were added in Bayer digestion as additives, the A/S ratios are 1.53, 1.10 and 1.07, respectively. The relative alumina recovery for reductive Bayer digestion is obviously higher than that for current Bayer digestion due to avoiding the formation of hydrogarnet. It is estimated that the reductive Bayer digestion can reduce bauxite consumption about 200 kg for 1 t alumina compared with current Bayer digestion with lime added.

3.5 Occurrence form of iron minerals in tailings

The reductive Bayer digestion and iron recovery from red mud can significantly reduce the red mud emission. For instance, the tailing in Exp. 3 is 4.25 g and thus reduces about 70%, compared with that of 13.76 in Exp. 1. Considering the fact that there is about 13% of iron in the tailing, the occurrence forms of iron minerals in tailing and concentrate were investigated by X-ray diffraction as shown in Fig. 15. The iron minerals in concentrate exist almost in the form of magnetite, while the tailing contains magnetite and hematite. Combined

with SEM analysis (Fig. 16), besides the increase of coercivity and the decrease of magnetism with the decrease of particle size, the magnetite in tailing cannot be recovered fully, which may be caused by the fine particles less than 5 μm adhered to DSP particles. EDX analyses further reveal that iron is combined with titanium in the fine bright white particles, but the concrete form of titanium iron compounds cannot be clarified from the X-ray diffraction patterns. Consequently, the research on reaction behavior of titanium and iron minerals should be investigated in detail to improve the transformation and separation of iron minerals.
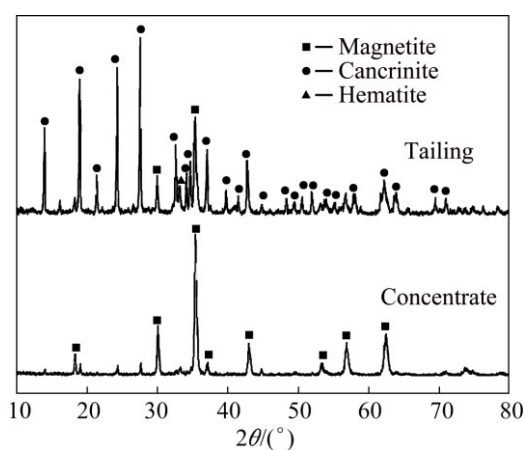
Fig. 15 XRD patterns of concentrate and tailing (Exp. 3 in Table 4)

4 Conclusions

1) The absolute value of zeta potential increases in order of hematite, magnetite and DSP, and wettability of minerals in polar solution increases in order of
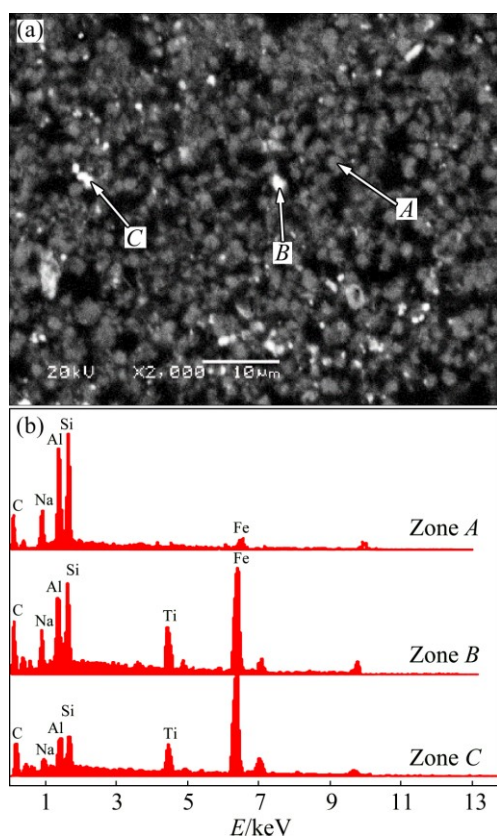
Fig. 16 SEM image (a) and EDX spectra (b) of tailing

magnetite, DSP and hematite, meanwhile the solvation trend increases in order of magnetite, hematite and DSP. Based on these differences, it was deduced that the conversion of hematite to magnetite in Bayer digestion favors the dissociation of iron and silicate minerals. This was verified experimentally using pure minerals.

2) In reductive Bayer digestion of high iron diasporic bauxite, increasing addition amount of iron powder and alkali concentration facilitates the conversion of hematite to magnetite. When addition amount of iron powder is 10% of bauxite, both the relative alumina recovery of 98.91% and complete conversion of hematite can be achieved simultaneously in digestion at 270 °C for 90 min with alkali concentration solution of 230 g/L and α_k of 3.0.

3) Processing RM-R can obtain qualified iron concentrate with iron grade of about 60% and recovery of 86.57% through magnetic separation, resulting in the reduction of red mud emission of about 70% compared with the current emission. A small fraction of magnetite entering the tailing may be caused by the fine-grain dissemination of iron and silicate minerals.

References

[1] SMITH P. Reactions of lime under high temperature Bayer digestion conditions [J]. Hydrometallurgy, 2017, 170: 16−23.

[2] XUE S G, ZHU F, KONG X F, WU C, HUANG L, HUANG N, HARTLEY W. A review of the characterization and revegetation of bauxite residues (red mud) [J]. Environmental Science and Pollution Research, 2016, 23(2): 1120−1132.

[3] KONG X F, LI M, XUE S G , HARTLEY W, CHEN C R, WU C, LI X F, LI Y W. Acid transformation of bauxite residue: Conversion of its alkaline characteristics [J]. Journal of Hazardous Materials, 2017, 324: 382−390.

[4] KAHN H, TASSINARI M M L, RATTI G. Characterization of bauxite fines aiming to minimize their iron content [J]. Minerals Engineering, 2003, 16: 1313−1315.

[5] BOLSAITIS P, CHANG V, SCHORIN H. Beneficiation of ferruginous bauxites by high-gradient magnetic separation [J]. International Journal of Mineral Processing, 1981, 8(3): 249−263.

[6] JAMIESON E, JONES A, COOLING D. Magnetic separation of red sand to produce value [J]. Minerals Engineering, 2006, 19: 1603−1605.

[7] LI Y R, WANG J, WANG X J. Feasibility study of iron mineral separation from red mud by high gradient superconducting magnetic separation [J]. Physica C: Superconductivity, 2011, 471: 91−96.

[8] WU X Q, XU P Y, DUAN Y F. Surface magnetization of siderite mineral [J]. International Journal of Mining Science & Technology, 2012, 22: 816−821.

[9] THELLA J S, MUKHERJEE A K, SRIKAKULAPU N G. Processing of high alumina iron ore slimes using classification and flotation [J]. Powder Technology, 2012, 217: 418−426.

[10] GUANG Jian-hong. Study on recovering Fe from red mud with SLon vertical ring and pulsating high gradient magnetic separator [J]. Jiangxi Nonferrous Metals, 2000, 14: 15−18. (in Chinese)

[11] LI X B, XIAO W, LIU W, LIU G H, PENG Z H, ZHOU Q S, QI T G. Recovery of alumina and ferric oxide from Bayer red mud rich in iron by reduction sintering [J]. Transactions of Nonferrous Metals Society of China, 2009, 19: 1342−1347.

[12] PICKLES C A, LU T, CHAMBERS B, FORSTER J. A study of reduction and magnetic separation of iron from high iron bauxite ore [J]. Canadian Metallurgical Quarterly, 2012, 51: 424−433.

[13] ERCAĞ E, APAK R. Furnace smelting and extractive metallurgy of red mud: Recovery of TiO_2, Al_2O_3 and pig iron [J]. Journal of Chemical Technology and Biotechnology, 1997, 70: 241−246.

[14] PIGA L, POCHETTI F, STOPPA L. Recovering metals from red mud generated during alumina production [J]. JOM, 1993, 45: 54−59.

[15] RAO R B, BESRA L, REDDY B R, BANERJEE G N. The effect of pretreatment on magnetic separation of ferruginous minerals in bauxite [J]. Magnetic and Electrical Separation, 1997, 8: 115−123.

[16] LIU W C, YANG J K, XIAO B. Application of Bayer red mud for iron recovery and building material production from alumosilicate residues [J]. Journal of Hazardous Materials, 2009, 161: 474−478.

[17] LI X B, YU S W, DONG W B, CHEN Y K, ZHOU Q S, QI T G, LIU G H, PENG Z H, JIANG Y Y. Investigating the effect of ferrous ion on the digestion of diasporic bauxite in the Bayer process [J]. Hydrometallurgy, 2015, 152: 183−189.

[18] LI X B, LIU N, QI T G, WANG Y L, ZHOU Q S, PENG Z H, LIU G H. Conversion of ferric oxide to magnetite by hydrothermal reduction in Bayer digestion process [J]. Transactions of Nonferrous Metals Society of China, 2015, 25: 3467−3474.

[19] LI Xiao-bin, ZHAO Dong-feng, ZHANG Xuan, LIU Gui-hua, PENG Zhi-hong, ZHOU Qiu-sheng. Effect of surface property of main minerals in red mud on their sedimentation ability [J]. Chinese Journal of Nonferrous Metals, 2012, 22: 281−286. (in Chinese)

[20] ZENG L M, LI Z B. Dissolution behavior of aluminum, silicon, and iron of diaspore concentrate in NaOH−NaAl(OH)₄ solutions at elevated temperature [J]. Industrial & Engineering Chemistry Research, 2013, 52: 18429−18439.

[21] ISHIKAWA K, YOSHIOKA T, SATO T, OKUWAKI A. Solubility of hematite in LiOH, NaOH and KOH solutions [J]. Hydrometallurgy, 1997, 45: 129−135.

[22] DIAKONOV I I, SCHOTT J, MARTIN F, HARRICHOURRY J C, ESCALIER J. Iron(III) solubility and speciation in aqueous solutions. Experimental study and modelling: Part 1. Hematite solubility from 60 to 300 °C in NaOH−NaCl solutions and thermodynamic properties of $Fe(OH)_4^-$ (aq) [J]. Geochimica et Cosmochimica Acta, 1999, 63: 2247−2261.

拜耳法还原溶出过程中赤铁矿的转化与铁的回收

李小斌，王一霖，周秋生，齐天贵，刘桂华，彭志宏，王洪阳

中南大学 冶金与环境学院，长沙 410083

摘　要：提出在拜耳法还原溶出过程中，添加铁粉作为还原剂实现铁矿物的定向转化；根据各矿物间表面性质差异完成铁矿物与钠硅渣(脱硅产物，DSP)的矿相解离。研究结果表明：磁铁矿与钠硅渣在 zeta 电位、润湿性和溶剂化趋势上的差异使其相对于赤铁矿更易于聚集长大和实现单体解离；采用还原拜耳法溶出处理高铁一水硬铝石型铝土矿时，提高还原剂添加量和溶液苛性碱浓度均有利于铁矿物的转化，同时氧化铝相对溶出率可达 98.91%；通过磁选分离还原溶出赤泥中的铁，可以获得铁精矿品位 TFe≈60%、矿石中铁回收率大于 86%、外排赤泥减少 70%的良好指标。研究结果有助于高效处理高铁一水硬铝石型铝土矿新技术的开发，也可为高铁赤泥的综合利用研究提供借鉴。

关键词：拜耳法溶出；还原；赤铁矿；磁铁矿；赤泥

(Edited by Wei-ping CHEN)